The cytoskeletal adapter protein 4.1G organizes the internodes in peripheral myelinated nerves

Aleksandra Ivanovic,[1] Ido Horresh,[3] Neev Golan,[3] Ivo Spiegel,[3] Helena Sabanay,[3] Shahar Frechter,[3] Shinichi Ohno,[4] Nobuo Terada,[4] Wiebke Möbius,[2] Jack Rosenbluth,[5] Nils Brose,[1] and Elior Peles[3]

[1]Department of Molecular Neurobiology and [2]Department of Neurogenetics, Max Planck Institute of Experimental Medicine, D-37075 Göttingen, Germany
[3]Department of Molecular Cell Biology, Weizmann Institute of Science, Rehovot 76100, Israel
[4]Department of Anatomy and Molecular Histology, Interdisciplinary Graduate School of Medicine and Engineering, University of Yamanashi, Chuo-City, Yamanashi 409-3898, Japan
[5]Department of Physiology and Neuroscience, New York University School of Medicine, New York, NY 10016

Myelinating Schwann cells regulate the localization of ion channels on the surface of the axons they ensheath. This function depends on adhesion complexes that are positioned at specific membrane domains along the myelin unit. Here we show that the precise localization of internodal proteins depends on the expression of the cytoskeletal adapter protein 4.1G in Schwann cells. Deletion of 4.1G in mice resulted in aberrant distribution of both glial adhesion molecules and axonal proteins that were present along the internodes. In wild-type nerves, juxtaparanodal proteins (i.e., Kv1 channels, Caspr2, and TAG-1) were concentrated throughout the internodes in a double strand that flanked paranodal junction components (i.e., Caspr, contactin, and NF155), and apposes the inner mesaxon of the myelin sheath. In contrast, in *4.1G*$^{-/-}$ mice, these proteins "piled up" at the juxtaparanodal region or aggregated along the internodes. These findings suggest that protein 4.1G contributes to the organization of the internodal axolemma by targeting and/or maintaining glial transmembrane proteins along the axoglial interface.

Introduction

Fast and efficient conduction along myelinated axons requires the precise positioning of ion channels and other proteins at distinct domains along the axolemma. These domains include the node of Ranvier, the paranodal junction (PNJ), the juxtaparanode (JXP), and the internodal region (Poliak and Peles, 2003; Hedstrom and Rasband, 2006; Salzer et al., 2008). The local differentiation of the axolemma depends on the function of cell adhesion molecules (CAMs) that are uniquely present at each domain. For example, clustering of Na^+ channels at the node is regulated by binding of the axonodal CAM neurofascin 186 (NF186) to gliomedin present at the Schwann cell microvilli (Eshed et al., 2005, 2007), as well as by the bordering PNJ, which maintains these channels at the nodal gap (Eshed et al., 2007; Feinberg et al., 2010). The PNJ forms between the paranodal loops of myelinating glia and the axon, and its formation is mediated by an adhesion complex consisting of Caspr, contactin, and the glial 155-kD isoform of neurofascin (NF155; Bhat et al., 2001; Boyle et al., 2001; Gollan et al., 2003; Sherman et al., 2005). The PNJ separates nodal Na^+ channels from Kv1 K^+ channels present at the JXP axolemma (Wang et al., 1993; Rhodes et al., 1997; Rasband et al., 1999; Vabnick et al., 1999). The accumulation of Kv1 channels at the JXP requires the presence of a Caspr-dependent membrane barrier at the PNJ (Bhat et al., 2001; Boyle et al., 2001; Gollan et al., 2003; Sherman et al., 2005), as well as a juxtaparanodal adhesion scaffold consisting of Caspr2 and TAG-1 (Poliak et al., 2003; Traka et al., 2003).

Throughout the internode, Kv1.2 is located in a double strand that apposes the inner mesaxon of the myelin sheath, and also forms a circumferential ring just below the Schmidt-Lanterman incisures (SLI; termed the juxtamesaxon; Arroyo et al., 1999). The juxtamesaxonal strands of Kv1.2 flank a single line of Caspr, which is reminiscent of the domain organization

A. Ivanovic, I. Horresh, and N. Golan contributed equally to this paper.

Correspondence to Elior Peles: peles@weizmann.ac.il

Abbreviations used in this paper: CAM, cell adhesion molecule; JXP, juxtaparanode; PNJ, paranodal junction; PNS, peripheral nervous system; SLI, Schmidt-Lanterman incisures.

The Rockefeller University Press $30.00
J. Cell Biol. Vol. 196 No. 3 337–344
www.jcb.org/cgi/doi/10.1083/jcb.201111127

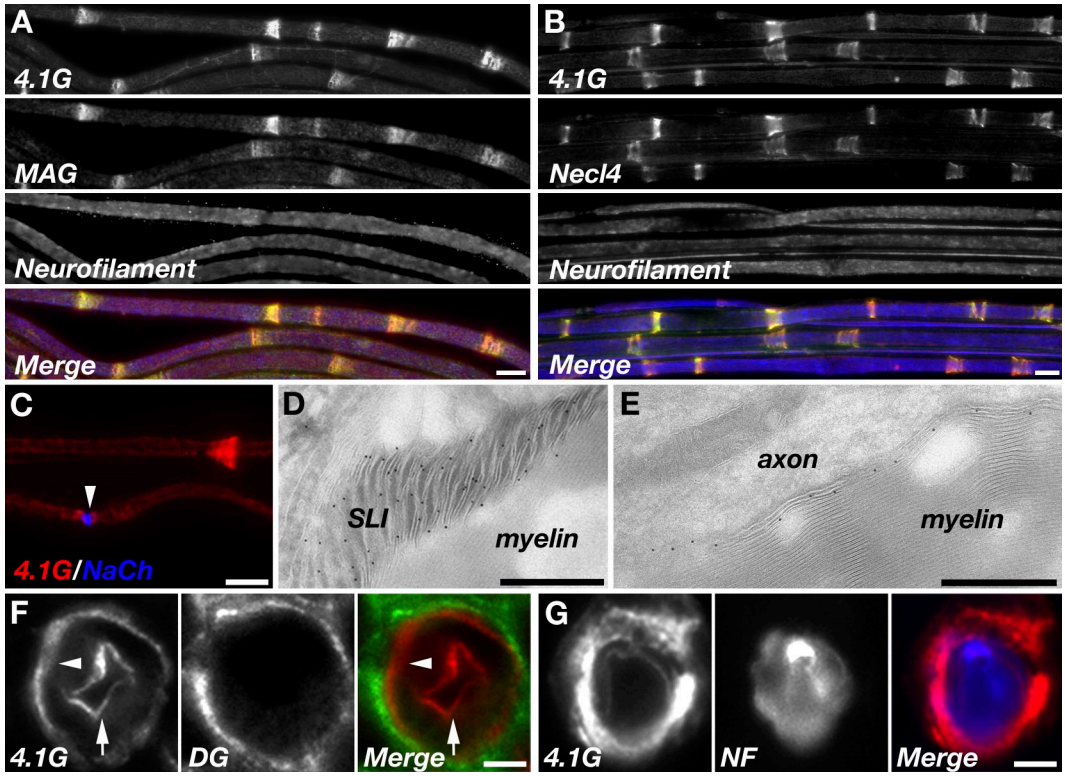

Figure 1. **4.1G colocalizes with Necl4 in myelinated peripheral nerves.** (A and B) Immunofluorescence labeling of teased adult mouse sciatic nerves using antibodies to protein 4.1G, neurofilament, and MAG (A) or Necl4 (B). (C) Double labeling of teased sciatic nerves for protein 4.1G and Na^+ channels. An arrowhead marks the location of the node. (D and E) Immunoelectron microscopy analysis of adult rat sciatic nerves using an antibody to protein 4.1G. Specific labeling is detected at the SLI (D), and along the adaxonal membrane (E). (F and G) Immunofluorescence labeling of sciatic nerve cross-sections using antibodies to protein 4.1G and dystroglycan (DG; F), or protein 4.1G and neurofilament (NF; G). The location of the adaxonal and abaxonal membranes is marked by arrows and arrowheads, respectively. Bars: (A–C) 10 µm; (D and E) 0.5 µm; (F and G) 5 µm.

around the nodes. However, juxtamesaxonal clustering of Kv1.2 still occurs in the absence of Caspr (Bhat et al., 2001) or Caspr2 (Poliak et al., 2003), which indicates that this membrane domain forms by a mechanism that is distinct from the ones operating at the PNJ and JXP. At the juxtamesaxonal line, Kv1 channels are found opposite to MAG (Arroyo et al., 1999) and Necl4 (Spiegel et al., 2007), two glial adhesion molecules that are enriched at the periaxonal membrane and inner mesaxon.

Caspr and Necl proteins bind to cytoskeletal adapters of the protein 4.1 family (Peles et al., 1997; Poliak et al., 1999; Gollan et al., 2002; Yageta et al., 2002; Denisenko-Nehrbass et al., 2003; Zhou et al., 2005; Hoy et al., 2009). These adapters play an important role in membrane organization by linking various transmembrane components, including ion channels (Li et al., 2007; Baines et al., 2009) and receptors (Binda et al., 2002; Lin et al., 2009), to the underlying actin/spectrin cytoskeleton (Bennett and Baines, 2001). For example, it was previously shown that the interaction between 4.1B and Caspr proteins is required to stabilize Caspr at the PNJ and to maintain Kv1 channels at the JXP (Gollan et al., 2002; Horresh et al., 2010; Buttermore et al., 2011; Cifuentes-Diaz et al., 2011). Protein 4.1 family consists of four members, of which three (4.1B, 4.1N, and 4.1R) are expressed by sensory neurons in the peripheral nervous system (PNS; Ohara et al., 2000; Poliak et al., 2001; Arroyo et al., 2004; Ogawa et al., 2006), whereas the fourth (4.1G) is expressed by myelinating Schwann cells (Horresh et al., 2010), where it is present at the periaxonal and mesaxonal membranes (Ohno et al., 2006). Here we report that protein 4.1G plays an essential role in the molecular organization of myelinated axons.

Results and discussion

Protein 4.1G is located at the axoglial interface in peripheral myelinated nerves

To examine whether protein 4.1G participates in the organization of the axoglial interface in myelinated nerves, we first compared its distribution with that of MAG and Necl4, two glial CAMs that are located at the periaxonal membrane and are thought to mediate Schwann cell–axon interaction (Trapp et al., 1989; Maurel et al., 2007; Spiegel et al., 2007). In agreement with a previous study (Ohno et al., 2006), protein 4.1G was detected together with MAG and Necl4 at the periaxonal membrane, as well as in regions of noncompact myelin such as the SLI and the paranodal loops (Fig. 1, A–C). The presence of protein 4.1G at the SLI and the periaxonal membrane was further demonstrated by immunoelectron microscopy (Fig. 1, D and E), as well as by immunolabeling of sciatic nerve cross sections (Fig. 1, F and G). These results show that protein 4.1G is positioned at the axoglial interface along the myelin unit, where it may link membrane proteins such as Necl4 to the underlying cytoskeleton.

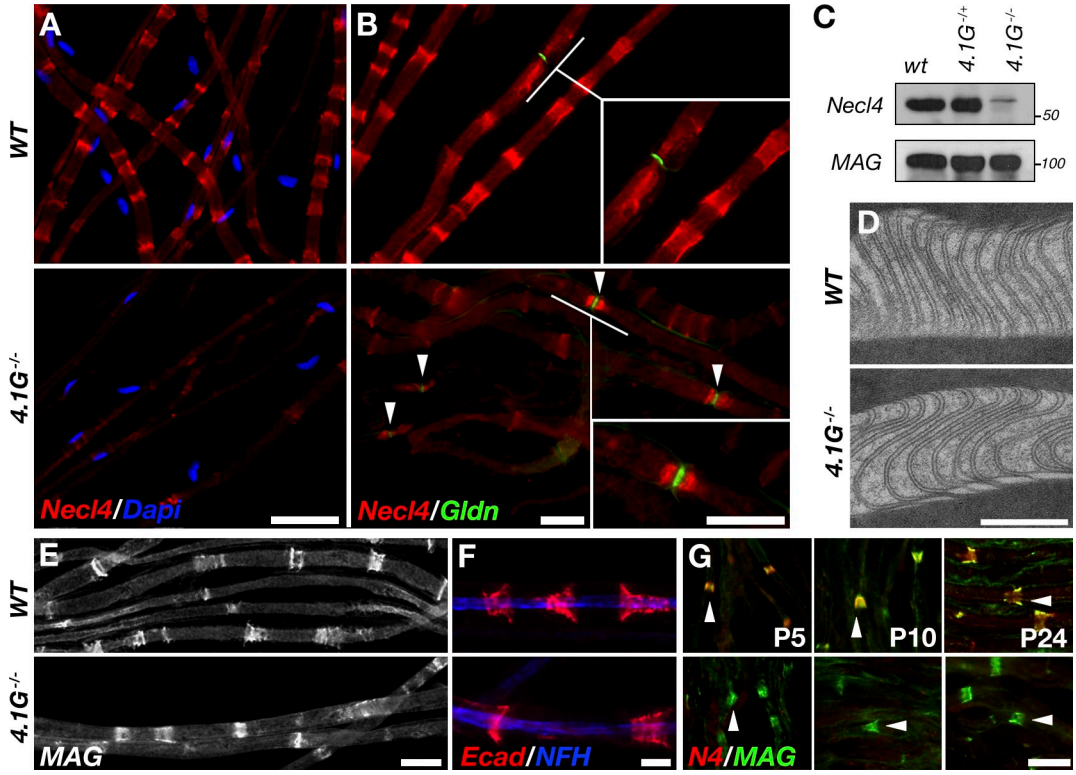

Figure 2. **Protein 4.1G is required for the expression of Necl4 at the axoglial interface.** (A and B) Necl4 immunolabeling of teased sciatic nerves isolated from WT mice or 4.1G-null mice (*4.1G*$^{-/-}$). Nuclei are labeled with Dapi (A). Immunolabeling of gliomedin (Gldn) was used to locate the nodes of Ranvier (B, arrowheads). Higher magnifications of the underlined areas are shown in the insets in each panel. Note the concentration of Necl4 at the paranodes flanking gliomedin-labeled nodes in the mutant. (C) Western blot analysis of sciatic nerve lysates isolated from WT, heterozygous (*4.1G*$^{-/+}$), and homozygous (*4.1G*$^{-/-}$) mice using antibodies to Necl4 and MAG. The location of molecular mass markers is shown on the right of each panel in kilodaltons. Note the reduced expression of Necl4 in the mutant. (D) Transmission electron microscopy images showing SLI in WT and *4.1G*-null mice (*4.1G*$^{-/-}$). (E and F) Immunofluorescence labeling of teased sciatic nerves isolated from WT or mutant mice using antibodies to MAG (E), or to E-Cadherin (Ecad) and neurofilament (NFH; F). (G) Immunolabeling of sciatic nerve sections of 5 (P5)-, 10 (P10)-, and 24 (P24)-d-old WT and *4.1G*$^{-/-}$ mice, using antibodies to Necl4 (N4) and MAG. One SLI in each panel is marked with an arrowhead. Bars: (A) 50 µm; (B) 20 µm; (D) 0.1 µm; (E and F) 20 µm; (G) 10 µm.

4.1G is required for the localization of Necl4 at the axoglial internodal interface

In view of the remarkable similarity in the localization of Necl4 and 4.1G in myelinating Schwann cells, the fact that 4.1 proteins bind members of the Necl family (Yageta et al., 2002; Zhou et al., 2005; Hoy et al., 2009), and the function of 4.1 proteins in membrane organization (Baines et al., 2009), we examined whether the localization of Necl4 is altered in the absence of protein 4.1G. In wild-type (WT) nerves, Necl4 immunoreactivity was detected in the SLI, the periaxonal (adaxonal) membrane, and detected weakly at the paranodal loops (Fig. 2, A and B), as anticipated from previous studies (Maurel et al., 2007; Spiegel et al., 2007). In contrast, in sciatic nerves isolated from *4.1G*$^{-/-}$ mice, there was a striking reduction in the level of Necl4 in the periaxonal membrane and the SLI (Fig. 2 A), which was accompanied by an abnormal concentration of Necl4 at the paranodal loops (Fig. 2, B and G). Western blot analysis of sciatic nerve lysates prepared from WT and *4.1G*$^{-/-}$ mice revealed that there was an ∼90% reduction in the amount of Necl4 in the mutant (Fig. 2 C), whereas the expression of MAG, which colocalized with Necl4 in myelinating Schwann cells (Maurel et al., 2007; Spiegel et al., 2007), was unchanged (Fig. 2, C and E). The reduction of Necl4 did not result from an impaired formation of the SLI, as their morphology in the mutant was indistinguishable from that seen in WT nerves (Fig. 2 D). Furthermore, immunolabeling of teased sciatic nerves using antibodies to other SLI proteins such as MAG and E-cadherin showed that in contrast to Necl4, these proteins were normally localized in the absence of protein 4.1G (Fig. 2, E and F). The marked reduction in Necl4 immunoreactivity at the SLI was already apparent at P5, as was evident by immunolabeling of sciatic nerves isolated at different developmental days, using antibodies to Necl4 and MAG (Fig. 2 G). Nevertheless, analysis of ultrathin sections of sciatic nerves by electron microscopy revealed no significant differences in myelin thickness (G ratio: WT, 0.57 ± 0.01; *4.1G*$^{-/-}$, 0.52 ± 0.04), axonal caliber (WT, 4.40 ± 0.3 µm; *4.1G*$^{-/-}$, 3.88 ± 0.7 µm), width of the periaxonal space (WT, 23 ± 4.0 nm; *4.1G*$^{-/-}$, 22.6 ± 4.0 nm), or periodicity of compact myelin between *4.1G*$^{-/-}$ and WT nerves (Fig. S1). Consistent with the observed normal morphology of the mutant, the levels of myelin proteins such as MBP, MAG, and P0 were not reduced in sciatic nerves of *4.1G*$^{-/-}$ mice (Fig. S1 I).

The specific requirement of 4.1G for the targeting of Necl4 within myelinating Schwann cells is in line with previous observations demonstrating that: (a) 4.1–Necl complexes exist in different subcellular structures (Terada et al., 2010; Nagata et al., 2011), (b) 4.1 proteins bind the cytoplasmic

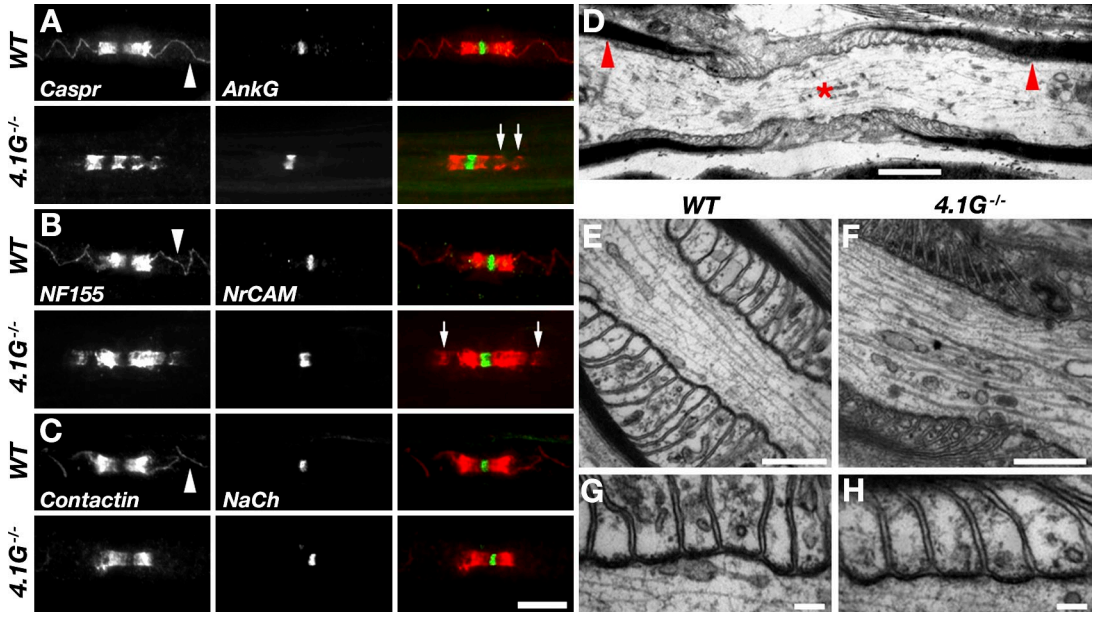

Figure 3. **Molecular composition of nodes and the PNJ in the absence of 4.1G.** (A–C) Immunofluorescence labeling of teased sciatic nerves isolated from WT mice and 4.1G-null mice (*4.1G*$^{-/-}$), using antibodies to Caspr and ankyrin G (AnkG; A), neurofascin 155 (NF155) and NrCAM (B), or contactin and Na^+ channels (NaCh; C). Merged images are shown on the right of each panel set. Arrowheads mark the presence of Caspr along the mesaxonal line, which projects from the PNJ in WT axons. Arrows mark the aberrant accumulation of Caspr (A) and NF155 (B) adjacent to the PNJ in the mutant nerve. (D–H) Transmission electron microscopy images of longitudinal sections of sciatic nerves from WT (E and G) and mutant (D, F, and H) mice. (D) A normal-appearing node (asterisk) in the mutant nerve lies between two paranodes, consisting of 18–19 overlapping terminal loops. Arrowheads mark the beginning of the PNJ. (G and H) Higher magnifications of the paranodal area showing that the mutant PNJ is indistinguishable from that seen in the WT control nerve. Bars: (A–C) 10 µm; (D–F) 0.5 µm; (G and H) 0.1 µm.

domain of Necls (Yageta et al., 2002; Zhou et al., 2005; Hoy et al., 2009), (c) the interaction between Necl4 and 4.1G is required for targeting and localization of Necl4 in Sertoli cells (Yang et al., 2011), and (d) the targeting of the MPP6 (MAGUK p55 subfamily member 6), a scaffolding protein that binds both 4.1G (Terada et al., 2011) and Necl proteins (Shingai et al., 2003; Kakunaga et al., 2005) to the SLI, requires 4.1G (Terada et al., 2011).

4.1G is required for the accurate localization of internodal adhesion complexes

We next examined whether the absence of protein 4.1G in Schwann cells, which results in the mislocalization of Necl4 along the internodal axoglial interface, also affects the molecular organization of the axon. Immunofluorescence analysis of teased sciatic nerves from WT and 4.1G$^{-/-}$ mice demonstrated that ankyrin G, NrCAM, and Na^+ channels were concentrated at the nodes of Ranvier in both genotypes (Fig. 3, A–C). Also, Caspr, contactin, and NF155 were present at both sides of the nodes (Fig. 3, A–C), which indicates that the PNJs are formed in the absence of protein 4.1G. This conclusion was further supported by transmission electron microscopic analysis of the mutant nerves, which showed the formation of the PNJ septa and a close (2–3 nm) association of the glial paranodal loops with the axolemma in mutant samples (Fig. 3, D–H). Nevertheless, although in WT axons Caspr, contactin, and NF155 were also present along the mesaxonal line that projects from the PNJ (arrowhead in Fig. 3 A), they were rarely detected at this location in the mutant nerve. In *4.1G*$^{-/-}$, but not in WT nerves, we often detected aberrant accumulation of Caspr and NF155 adjacent to the PNJ (arrows in Fig. 3, A and B). We also compared the distribution of NF155 and Caspr in sciatic nerves isolated from WT and 4.1G mutant at early postnatal days (i.e., P3, P5) and found that these two proteins are always found together in the mutant, making it impossible to determine whether glial components accumulation at paranodes preceded that of axonal ones (unpublished data).

Absence of 4.1G results in aberrant axonal clustering of Kv1

Immunofluorescence labeling of teased sciatic nerves isolated from WT and 4.1G$^{-/-}$ mice using antibodies to Caspr2, Kv1.2, and TAG-1, revealed that these proteins abnormally "piled up" at the mutant JXP (Fig. 4, A–C). In contrast to WT mice, where Kv1.2 was present along the internodes in a double strand that apposes the inner mesaxon of the myelin sheath (Fig. 4 D, top), in the absence of protein 4.1G these channels redistributed from the internodes toward the JXP and were occasionally detected in small aggregates along the internodes (Fig. 4 D). Western blot analysis of sciatic nerve lysates demonstrated that *4.1G*$^{-/-}$ mutant nerves contained normal levels of Caspr and Kv1.2 channels, further supporting the conclusion that these proteins were relocated from the internodes toward the paranodes. Abnormal accumulation of Kv1 channels was already detected at P12 in *4.1G*$^{-/-}$ nerves, which suggests that it represents an early developmental defect (Fig. 4 F). In agreement with previous developmental studies (Vabnick et al., 1999; Poliak et al., 2001), at earlier time points (P10), Kv1.2 was detected at the PNJ and JXP in both WT and *4.1G*$^{-/-}$ nerves. Electrophysiological analysis of sciatic nerves isolated from adult WT and *4.1G*$^{-/-}$ mice revealed that

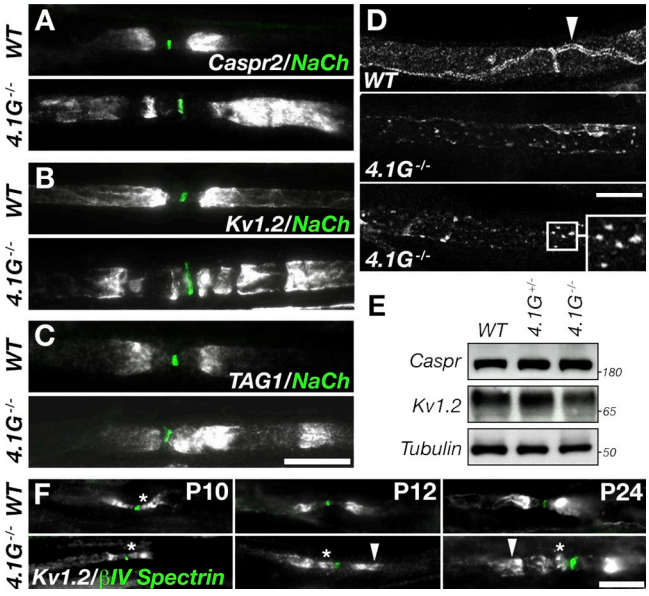

Figure 4. **Protein 4.1G is essential for the molecular organization of the internode.** (A–C) Double immunofluorescence labeling of teased sciatic nerves isolated from WT mice and 4.1G-null mice (*4.1G*$^{-/-}$), using antibodies to Na^+ channels (NaCh) and Caspr2 (A), Kv1.2 (B), or TAG-1 (C). In 4.1G-null nerves, Caspr2 and Kv1 channels were aberrantly concentrated at the JXP and adjacent area (A and B), whereas glial TAG-1 is also detected at the paranodes (C). (D) Immunolabeling of teased sciatic nerves from WT and 4.1G mutant mice, using an antibody to Kv1.2. In WT nerves, internodal Kv1.2 immunoreactivity is detected in a double mesaxonal line (arrowhead), whereas in the absence of protein 4.1G they are often detected in aggregates (inset in the bottom panel). (E) 4.1G mutant nerves contain normal amounts of Caspr and Kv1.2. Western blot analysis of sciatic nerve lysates isolated from WT, heterozygous (*4.1G*$^{+/-}$), and homozygous 4.1G-null mice (*4.1G*$^{-/-}$) using antibodies to Caspr, Kv1.2 channel, or β-tubulin. The location of molecular mass markers is shown on the right of each panel in kilodaltons. (F) Immunolabeling of sciatic nerve sections from WT and 4.1G mutant mice, using an antibody to Kv1.2 and βIV-spectrin. At P10, Kv1.2 immunoreactivity is detected at the PNJ (asterisks) in both WT and mutant (*4.1G*$^{-/-}$) mice. Abnormal accumulation of Kv1.2 at the edge of the JXP (arrowheads) is detected at P12 and P24 in the mutant. Bars: (A–C) 15 µm; (D and F) 10 µm.

both genotypes have similar nerve conduction velocities (WT, 39.6 ± 0.7 m/s; mutant, 40.4 ± 5 m/s), which is likely due to the fact that although these channels are abnormally clustered, they are still concealed under the compact myelin in the mutant (Vabnick et al., 1999; Poliak et al., 2003).

4.1G$^{-/-}$ defines a novel internodal phenotype

The distribution of ion channels along myelinated axons is critically dependent on Schwann cells and represents a sensitive indicator of myelin abnormalities (Dupree et al., 1999; Poliak et al., 2001; Arroyo et al., 2004; Lonigro and Devaux, 2009). The precise positioning of these channels at the axolemma is regulated by their association with axoglial CAMs and cytoskeleton-linker proteins (Susuki and Rasband, 2008). In peripheral myelinated axons, Kv1 channels are present in the JXP and in the juxtamesaxonal lines that run through the internodes (Wang et al., 1993; Arroyo et al., 1999). At these sites, Kv1 channels are well positioned to act as active dampers of reentrant excitation, and help in maintaining the internodal resting potential (Chiu, 1980; Chiu and Ritchie, 1984; Zhou et al., 1998; Vabnick et al., 1999). Our results indicate that the mechanisms underlying the clustering of Kv1 channels at the JXP and the internodal axolemma are likely to be distinct (Fig. 5). Juxtaparanodal clustering of Kv1 channels depends on both the formation of a membrane barrier at the PNJ and the generation of a juxtaparanodal adhesion scaffolding complex by Caspr2 and TAG-1 (Poliak and Peles, 2003; Salzer et al., 2008). Although Kv1 channels aberrantly accumulate immediately adjacent to the nodes in peripheral nerves of mutants lacking Caspr (Bhat et al., 2001; Gollan et al., 2003), contactin (Boyle et al., 2001), NF155 (Pillai et al., 2009), or ceramide galactosyltransferase (*cgt*; Dupree et al., 1999), they are still present at the internodal juxtamesaxonal lines in these mutants (Fig. 5 B). Similarly, in mutants with juxtaparanodal aberrations such as mice lacking Caspr2 (Poliak et al., 2003), TAG-1 (Poliak et al., 2003; Traka et al., 2003), or protein 4.1B (Horresh et al., 2010), Kv1 channels do not cluster at the JXP and mainly concentrate at the juxtamesaxonal lines (Fig. 5 C). In the present study, we found that the localization of Kv1 channels along the mesaxonal line depends on the expression of protein 4.1G in myelinating Schwann cells. In the absence of protein 4.1G, the overall level of Kv1 channels is unchanged, but they aberrantly "pile up" at the JXP and aggregate along the internodal axolemma (Fig. 5 D). Notably, in the absence of 4.1G, both Caspr and Caspr2 are not localized at the juxtamesaxonal line, indicating that the clustering of Kv1 channels

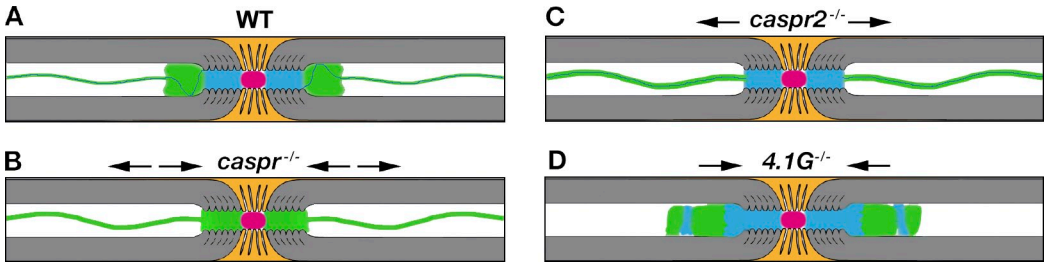

Figure 5. **Mice lacking protein 4.1G define a novel internodal phenotype.** A schematic drawing illustrating the molecular organization of myelinated PNS axons in WT (A), paranodal mutant (B; *caspr*, *cgt*, *contactin*, and *NF155*), juxtaparanodal mutant (C; *caspr2*, *tag1*, and *4.1B*), and internodal mutant (D; *4.1G*). In WT nerves, Na^+ channel (red) clusters at the nodes are separated from juxtaparanodal Kv1 channels (green) by Caspr-labeled (blue) PNJ. Kv1 channels are also located in a double line bordering a single line of Caspr along the internodes (termed the juxtamesaxon). In the absence of Caspr, Kv1 channels are located at the paranodes and the juxtamesaxonal lines, whereas in Caspr2-null nerves these channels redistribute (arrows) from the JXP to the juxtamesaxonal lines. In contrast, deletion of protein 4.1G results in the disappearance of both Caspr and kv1 channels from the internodal lines and their aberrant accumulation at the juxtaparanodal region.

at this site requires the presence of at least one of the two Caspr proteins.

We thus propose that two membrane barriers that are present at both the PNJ and the juxtamesaxonal line regulate the clustering of Kv1 channels in peripheral myelinated axons. Although the PNJ barrier controls the axial (longitudinal) distribution of Kv1 channels, the presence of this membrane barrier at the juxtamesaxonal line affects the distribution of these channels around the axon circumference (radial). In the absence of the PNJ barrier in Caspr-deficient nerves, Kv1 channels are still trapped at the juxtamesaxonal line by Caspr2, whereas in Caspr2-deficient axons, these channels are located at the juxtamesaxonal line because of the presence of the Caspr-mediated membrane barrier at this site. In contrast, in 4.1G$^{-/-}$ nerves, both the juxtamesaxonal NF155/Caspr-dependent membrane barrier and the TAG-1/Caspr2-dependent scaffold are missing, resulting in the diffusion of Kv1 channels away from the mesaxonal line. In these axons, Kv1 channels are mainly accumulated by Caspr2 at the JXP, which is formed near a Caspr-dependent membrane barrier at the PNJ. Our findings suggest that protein 4.1G plays an important role in the polarized distribution of proteins in myelinating Schwann cells, which is required for the precise molecular organization of the underlying axonal membrane.

Materials and methods

Mice

Generation of 4.1G$^{-/-}$ mice was achieved by replacing the first coding exon with a neomycin selection cassette as described previously (Wozny et al., 2009). Genotyping was done by PCR of genomic tail DNA using primers: 5′-TTTCCATCACCTCACCACCAGACTG-3′ and 5′-CACTTCAGATGCAGAGCCAACTTCAG-3′ or 5′-ATTAAAGGGCCTGGCAAGGTCAAC-3′ and 5′-CCTCCCCTACCCGGTAGAATTGG-3′ for WT and mutant alleles, respectively. WT control animals were derived from the same litters as mutants. Unless indicated otherwise, all histological analyses (immunohistochemistry and electron microscopy) were performed using 3–5 adult (3-mo-old) mice of each genotype. Figures show examples of the results that were reproducible and consistent between individual mice. All experiments were performed in compliance with the relevant laws and institutional guidelines of the Weizmann Institute's Institutional Animal Care and Use Committee, the Max Planck Society, and the State of Lower Saxony. Sciatic nerve conduction velocity measurements were performed on three animals of each genotype essentially as described previously (Eshed et al., 2007; Feinberg et al., 2010). In short, sciatic nerves were placed in a recording chamber and the ends of the nerves were drawn into suction electrodes for stimulation and recording of compound action potentials. Signals were amplified, digitized, recorded, and analyzed on a laboratory computer using pClamp10 program (Molecular Devices).

Antibodies

Polyclonal antibodies against 4.1G were generated by immunizing rabbits with a GST fusion protein containing amino acids 673–837 of human 4.1G (GenBank accession no. AF027299.1). Guinea pig antibodies against protein 4.1G were raised against a His-tagged protein containing amino acids 27–151 of mouse 4.1G (GenBank accession no. AJ542537). Specificity and cross-reactivity of these antibodies to 4.1G, 4.1B, 4.1R, and 4.1N were determined by immunostaining of COS-7 cells transfected with the relevant cDNAs (Horresh et al., 2010), as well as by staining nerves isolated from mice lacking 4.1G. Antibodies against P0 (Wong and Filbin, 1994), NrCAM (Lustig et al., 2001), and βIV-spectrin (Ogawa et al., 2010) were generously provided by M. Filbin (Hunter College, New York, NY), M. Grumet (Rutgers University, New Brunswick, NJ), and M. Rasband (Baylor College of Medicine, Houston, TX), respectively. Antibodies against Necl4 (Spiegel et al., 2007), Caspr (Peles et al., 1997), NF155 (Gollan et al., 2003), and contactin (Rios et al., 2000) have been described previously. Commercially available antibodies used in this study were as follows: rat anti-neurofilament clone TA51 (Millipore), mouse monoclonal antibodies against Kv1.1 (K20/78) and Kv1.2 (K14/16; NeuroMab), mouse anti-β dystroglycan (Novocastra), mouse anti-MAG clone 513 (Roche), mouse anti–E-cadherin (BD), mouse anti–ankyrin G (Santa Cruz Biotechnology, Inc.), mouse anti-Na^+ channels and mouse anti-MBP (Sigma-Aldrich), mouse anti-neurofilament (SMI-311R; Covance), and mouse anti-phosphorylated neurofilament (SMI-312R; Covance).

Immunolabeling and Western blot analysis

Sciatic nerves were dissected and immersed in freshly made 4% paraformaldehyde for 30 min at 4°C, or for 10 min in Zamboni's fixative at ambient temperature. Fixation of sciatic nerves for immunostaining with polyclonal antibodies against NF155 has been described previously (Tait et al., 2000). Nerves were teased on Super-Frost Plus slides, air-dried for 2–3 h, and then kept frozen at −20°C until used. Slides were postfixed using ice-cold methanol for 5 min, washed with PBS, and blocked for 1 h with blocking buffer (PBS containing 5% normal goat serum, 0.1% Triton X-100, and 0.1% glycine). The samples were incubated overnight at 4°C with the different primary antibodies diluted in blocking solution. Detection of primary antibodies was done using anti–mouse-Cy3, anti–rat-Cy5, anti–chicken-647 (Jackson ImmunoResearch Laboratories, Inc.), Alexa Fluor 555 goat anti–guinea pig (Molecular Probes), or anti–rabbit Alexa Fluor 488 (Invitrogen). Slides were mounted in Elvanol. Fluorescence images were obtained using a microscope (Axioskop 2; Carl Zeiss) equipped with 10×/0.3 Ph1, 20×/0.5 NA, 40×/1.3 NA, and 63×/1.4 NA Plan Neofluar objective lens, or using a confocal laser-scanning microscope (Zeiss 510; Carl Zeiss). Images were acquired using a charge-coupled device camera (ORCA-ER; Hamamatsu Photonics) controlled by acquisition software (Axiovision 4.7, or LSM 510 software; Carl Zeiss). Processing of the images was performed using Photoshop software (CS3; Adobe). Quantification of the myelin was performed using image analysis software (Volocity 4.2.1; PerkinElmer). Comparison of protein expression in sciatic nerves by Western blotting was done essentially as described previously (Horresh et al., 2010). Nerves were desheathed in cold PBS; frozen in liquid nitrogen; ground with a mortar and pestle; solubilized in a buffer containing 25 mM Tris, pH 8.0, 1 mM EDTA, and 2% SDS; and boiled for 15 min before being loaded on the gel.

Electron microscopy

Mice were perfused with 2.5% glutaraldehyde and 4% PFA in phosphate buffer as described previously (Möbius et al., 2010). Sciatic nerve specimens were embedded in epoxy resin (Serva GmbH). Ultrathin sections (50–70 nm) were cut on an ultramicrotome and collected on copper grids, stained with an aqueous solution of 4% uranyl acetate followed by lead citrate, or aqueous $KMnO_4$ followed by alcoholic uranyl acetate, and observed using a H-7500 transmission electron microscope (Hitachi), a LEO EM912 (Carl Zeiss), or a CX 100 transmission electron microscope (JEOL Ltd.). For electron microscopy of high-pressure frozen samples, sciatic nerves were cryofixed in a high-pressure freezer (HPM010; Bal-Tec). Freeze-substitution was performed in a Freeze Substitution and low-temperature embedding system (AFS; Leica) using the tannic acid–OsO4 protocol (Möbius et al., 2010). Samples were embedded in epon, sectioned using an Ultracut S ultramicrotome (Leica), and stained with an aqueous solution of 2% uranyl acetate followed by lead citrate. Cryo-immunoelectron microscopy was done as described previously (Werner et al., 2007; Golan et al., 2008). Grids were incubated with anti-4.1G antibody in blocking buffer, washed with PBS, and incubated with colloidal protein A–gold in blocking buffer (10 nm; Cell Microscopy Center, Department of Cell Biology, University Medical Center at Utrecht). Sections were postfixed with 1% glutaraldehyde, contrasted with neutral uranyl acetate (2% in 1.5 M oxalic acid, pH adjusted to 7.0 with ammonium hydroxide), and embedded in 1.8% methylcellulose containing 0.4% uranyl acetate. The sections were viewed in an electron microscope (LEO EM 912AB; Zeiss), and pictures were taken with an on-axis 2,048 × 2,048 charge-coupled device camera (ProScan). G ratio was calculated from at least 100 randomly chosen fibers per animal (n = 3 per genotype). Measurements of the periaxonal space in sciatic nerve sections were taken from WT and *4.1G*$^{-/-}$ mice (sampling every axon at four constant sites; 20 axons per mouse; n = 3 mice per genotype).

Online supplemental material

Fig. S1 shows the normal appearance of PNS myelin in mice lacking protein 4.1G. Online supplemental material is available at http://www.jcb.org/cgi/content/full/jcb.201111127/DC1.

We thank Orly Laufman for her assistance in obtaining confocal images.

This work was supported by the Minerva Foundation, National Institutes of Health (NS50220 to E. Peles and NS37475 to J. Rosenbluth), the National Multiple Sclerosis Society (grant RG3618), the Israel Science Foundation, the Max Planck Society, and the Moskowitz Center for Bio-Nano Imaging at the Weizmann Institute. E. Peles is the Incumbent of the Hanna Hertz Professorial Chair for Multiple Sclerosis and Neuroscience.

Submitted: 28 November 2011
Accepted: 31 December 2011

References

Arroyo, E.J., Y.T. Xu, L. Zhou, A. Messing, E. Peles, S.Y. Chiu, and S.S. Scherer. 1999. Myelinating Schwann cells determine the internodal localization of Kv1.1, Kv1.2, Kvbeta2, and Caspr. *J. Neurocytol.* 28:333–347. http://dx.doi.org/10.1023/A:1007009613484

Arroyo, E.J., E.E. Sirkowski, R. Chitale, and S.S. Scherer. 2004. Acute demyelination disrupts the molecular organization of peripheral nervous system nodes. *J. Comp. Neurol.* 479:424–434. http://dx.doi.org/10.1002/cne.20321

Baines, A.J., P.M. Bennett, E.W. Carter, and C. Terracciano. 2009. Protein 4.1 and the control of ion channels. *Blood Cells Mol. Dis.* 42:211–215. http://dx.doi.org/10.1016/j.bcmd.2009.01.016

Bennett, V., and A.J. Baines. 2001. Spectrin and ankyrin-based pathways: metazoan inventions for integrating cells into tissues. *Physiol. Rev.* 81: 1353–1392.

Bhat, M.A., J.C. Rios, Y. Lu, G.P. Garcia-Fresco, W. Ching, M. St Martin, J. Li, S. Einheber, M. Chesler, J. Rosenbluth, et al. 2001. Axon-glia interactions and the domain organization of myelinated axons requires neurexin IV/Caspr/Paranodin. *Neuron*. 30:369–383. http://dx.doi.org/10.1016/S0896-6273(01)00294-X

Binda, A.V., N. Kabbani, R. Lin, and R. Levenson. 2002. D2 and D3 dopamine receptor cell surface localization mediated by interaction with protein 4.1N. *Mol. Pharmacol.* 62:507–513. http://dx.doi.org/10.1124/mol.62.3.507

Boyle, M.E., E.O. Berglund, K.K. Murai, L. Weber, E. Peles, and B. Ranscht. 2001. Contactin orchestrates assembly of the septate-like junctions at the paranode in myelinated peripheral nerve. *Neuron*. 30:385–397. http://dx.doi.org/10.1016/S0896-6273(01)00296-3

Buttermore, E.D., J.L. Dupree, J. Cheng, X. An, L. Tessarollo, and M.A. Bhat. 2011. The cytoskeletal adaptor protein band 4.1B is required for the maintenance of paranodal axoglial septate junctions in myelinated axons. *J. Neurosci.* 31:8013–8024. http://dx.doi.org/10.1523/JNEUROSCI.1015-11.2011

Chiu, S.Y. 1980. Asymmetry currents in the mammalian myelinated nerve. *J. Physiol.* 309:499–519.

Chiu, S.Y., and J.M. Ritchie. 1984. On the physiological role of internodal potassium channels and the security of conduction in myelinated nerve fibres. *Proc. R. Soc. Lond. B Biol. Sci.* 220:415–422. http://dx.doi.org/10.1098/rspb.1984.0010

Cifuentes-Diaz, C., F. Chareyre, M. Garcia, J. Devaux, M. Carnaud, G. Levasseur, M. Niwa-Kawakita, S. Harroch, J.A. Girault, M. Giovannini, and L. Goutebroze. 2011. Protein 4.1B contributes to the organization of peripheral myelinated axons. *PLoS ONE*. 6:e25043. http://dx.doi.org/10.1371/journal.pone.0025043

Denisenko-Nehrbass, N., K. Oguievetskaia, L. Goutebroze, T. Galvez, H. Yamakawa, O. Ohara, M. Carnaud, and J.A. Girault. 2003. Protein 4.1B associates with both Caspr/paranodin and Caspr2 at paranodes and juxtaparanodes of myelinated fibres. *Eur. J. Neurosci.* 17:411–416. http://dx.doi.org/10.1046/j.1460-9568.2003.02441.x

Dupree, J.L., J.A. Girault, and B. Popko. 1999. Axo-glial interactions regulate the localization of axonal paranodal proteins. *J. Cell Biol.* 147:1145–1152. http://dx.doi.org/10.1083/jcb.147.6.1145

Eshed, Y., K. Feinberg, S. Poliak, H. Sabanay, O. Sarig-Nadir, I. Spiegel, J.R. Bermingham Jr., and E. Peles. 2005. Gliomedin mediates Schwann cell-axon interaction and the molecular assembly of the nodes of Ranvier. *Neuron*. 47:215–229. http://dx.doi.org/10.1016/j.neuron.2005.06.026

Eshed, Y., K. Feinberg, D.J. Carey, and E. Peles. 2007. Secreted gliomedin is a perinodal matrix component of peripheral nerves. *J. Cell Biol.* 177:551–562. http://dx.doi.org/10.1083/jcb.200612139

Feinberg, K., Y. Eshed-Eisenbach, S. Frechter, V. Amor, D. Salomon, H. Sabanay, J.L. Dupree, M. Grumet, P.J. Brophy, P. Shrager, and E. Peles. 2010. A glial signal consisting of gliomedin and NrCAM clusters axonal Na+ channels during the formation of nodes of Ranvier. *Neuron*. 65:490–502. http://dx.doi.org/10.1016/j.neuron.2010.02.004

Golan, N., K. Adamsky, E. Kartvelishvily, D. Brockschnieder, W. Möbius, I. Spiegel, A.D. Roth, C.E. Thomson, G. Rechavi, and E. Peles. 2008. Identification of Tmem10/Opalin as an oligodendrocyte enriched gene using expression profiling combined with genetic cell ablation. *Glia*. 56:1176–1186. http://dx.doi.org/10.1002/glia.20688

Gollan, L., H. Sabanay, S. Poliak, E.O. Berglund, B. Ranscht, and E. Peles. 2002. Retention of a cell adhesion complex at the paranodal junction requires the cytoplasmic region of Caspr. *J. Cell Biol.* 157:1247–1256. http://dx.doi.org/10.1083/jcb.200203050

Gollan, L., D. Salomon, J.L. Salzer, and E. Peles. 2003. Caspr regulates the processing of contactin and inhibits its binding to neurofascin. *J. Cell Biol.* 163:1213–1218. http://dx.doi.org/10.1083/jcb.200309147

Hedstrom, K.L., and M.N. Rasband. 2006. Intrinsic and extrinsic determinants of ion channel localization in neurons. *J. Neurochem.* 98:1345–1352. http://dx.doi.org/10.1111/j.1471-4159.2006.04001.x

Horresh, I., V. Bar, J.L. Kissil, and E. Peles. 2010. Organization of myelinated axons by Caspr and Caspr2 requires the cytoskeletal adapter protein 4.1B. *J. Neurosci.* 30:2480–2489. http://dx.doi.org/10.1523/JNEUROSCI.5225-09.2010

Hoy, J.L., J.R. Constable, S. Vicini, Z. Fu, and P. Washbourne. 2009. SynCAM1 recruits NMDA receptors via protein 4.1B. *Mol. Cell. Neurosci.* 42:466–483. http://dx.doi.org/10.1016/j.mcn.2009.09.010

Kakunaga, S., W. Ikeda, S. Itoh, M. Deguchi-Tawarada, T. Ohtsuka, A. Mizoguchi, and Y. Takai. 2005. Nectin-like molecule-1/TSLL1/SynCAM3: a neural tissue-specific immunoglobulin-like cell-cell adhesion molecule localizing at non-junctional contact sites of presynaptic nerve terminals, axons and glia cell processes. *J. Cell Sci.* 118:1267–1277. http://dx.doi.org/10.1242/jcs.01656

Li, H., S. Khirug, C. Cai, A. Ludwig, P. Blaesse, J. Kolikova, R. Afzalov, S.K. Coleman, S. Lauri, M.S. Airaksinen, et al. 2007. KCC2 interacts with the dendritic cytoskeleton to promote spine development. *Neuron*. 56:1019–1033. http://dx.doi.org/10.1016/j.neuron.2007.10.039

Lin, D.T., Y. Makino, K. Sharma, T. Hayashi, R. Neve, K. Takamiya, and R.L. Huganir. 2009. Regulation of AMPA receptor extrasynaptic insertion by 4.1N, phosphorylation and palmitoylation. *Nat. Neurosci.* 12:879–887. http://dx.doi.org/10.1038/nn.2351

Lonigro, A., and J.J. Devaux. 2009. Disruption of neurofascin and gliomedin at nodes of Ranvier precedes demyelination in experimental allergic neuritis. *Brain*. 132:260–273. http://dx.doi.org/10.1093/brain/awn281

Lustig, M., L. Erskine, C.A. Mason, M. Grumet, and T. Sakurai. 2001. Nr-CAM expression in the developing mouse nervous system: ventral midline structures, specific fiber tracts, and neuropilar regions. *J. Comp. Neurol.* 434:13–28. http://dx.doi.org/10.1002/cne.1161

Maurel, P., S. Einheber, J. Galinska, P. Thaker, I. Lam, M.B. Rubin, S.S. Scherer, Y. Murakami, D.H. Gutmann, and J.L. Salzer. 2007. Nectin-like proteins mediate axon Schwann cell interactions along the internode and are essential for myelination. *J. Cell Biol.* 178:861–874. http://dx.doi.org/10.1083/jcb.200705132

Möbius, W., B. Cooper, W.A. Kaufmann, C. Imig, T. Ruhwedel, N. Snaidero, A.S. Saab, and F. Varoqueaux. 2010. Electron microscopy of the mouse central nervous system. *Methods Cell Biol.* 96:475–512. http://dx.doi.org/10.1016/S0091-679X(10)96020-2

Nagata, M., M. Sakurai-Yageta, D. Yamada, A. Goto, A. Ito, H. Fukuhara, H. Kume, T. Morikawa, M. Fukayama, Y. Homma, and Y. Murakami. 2011. Aberrations of a cell adhesion molecule CADM4 in renal clear cell carcinoma. *Int. J. Cancer*. In press.

Ogawa, Y., D.P. Schafer, I. Horresh, V. Bar, K. Hales, Y. Yang, K. Susuki, E. Peles, M.C. Stankewich, and M.N. Rasband. 2006. Spectrins and ankyrinB constitute a specialized paranodal cytoskeleton. *J. Neurosci.* 26:5230–5239. http://dx.doi.org/10.1523/JNEUROSCI.0425-06.2006

Ogawa, Y., J. Oses-Prieto, M.Y. Kim, I. Horresh, E. Peles, A.L. Burlingame, J.S. Trimmer, D. Meijer, and M.N. Rasband. 2010. ADAM22, a Kv1 channel-interacting protein, recruits membrane-associated guanylate kinases to juxtaparanodes of myelinated axons. *J. Neurosci.* 30:1038–1048. http://dx.doi.org/10.1523/JNEUROSCI.4661-09.2010

Ohara, R., H. Yamakawa, M. Nakayama, and O. Ohara. 2000. Type II brain 4.1 (4.1B/KIAA0987), a member of the protein 4.1 family, is localized to neuronal paranodes. *Brain Res. Mol. Brain Res.* 85:41–52. http://dx.doi.org/10.1016/S0169-328X(00)00233-3

Ohno, N., N. Terada, H. Yamakawa, M. Komada, O. Ohara, B.D. Trapp, and S. Ohno. 2006. Expression of protein 4.1G in Schwann cells of the peripheral nervous system. *J. Neurosci. Res.* 84:568–577. http://dx.doi.org/10.1002/jnr.20949

Peles, E., M. Nativ, M. Lustig, M. Grumet, J. Schilling, R. Martinez, G.D. Plowman, and J. Schlessinger. 1997. Identification of a novel contactin-associated transmembrane receptor with multiple domains implicated in protein-protein interactions. *EMBO J.* 16:978–988. http://dx.doi.org/10.1093/emboj/16.5.978

Pillai, A.M., C. Thaxton, A.L. Pribisko, J.G. Cheng, J.L. Dupree, and M.A. Bhat. 2009. Spatiotemporal ablation of myelinating glia-specific neurofascin (Nfasc NF155) in mice reveals gradual loss of paranodal axoglial junctions and concomitant disorganization of axonal domains. *J. Neurosci. Res.* 87:1773–1793. http://dx.doi.org/10.1002/jnr.22015

Poliak, S., and E. Peles. 2003. The local differentiation of myelinated axons at nodes of Ranvier. *Nat. Rev. Neurosci.* 4:968–980. http://dx.doi.org/10.1038/nrn1253

Poliak, S., L. Gollan, R. Martinez, A. Custer, S. Einheber, J.L. Salzer, J.S. Trimmer, P. Shrager, and E. Peles. 1999. Caspr2, a new member of the neurexin superfamily, is localized at the juxtaparanodes of myelinated axons and associates with K+ channels. *Neuron*. 24:1037–1047. http://dx.doi.org/10.1016/S0896-6273(00)81049-1

Poliak, S., L. Gollan, D. Salomon, E.O. Berglund, R. Ohara, B. Ranscht, and E. Peles. 2001. Localization of Caspr2 in myelinated nerves depends on axon-glia interactions and the generation of barriers along the axon. *J. Neurosci.* 21:7568–7575.

Poliak, S., D. Salomon, H. Elhanany, H. Sabanay, B. Kiernan, L. Pevny, C.L. Stewart, X. Xu, S.Y. Chiu, P. Shrager, et al. 2003. Juxtaparanodal clustering of Shaker-like K+ channels in myelinated axons depends on Caspr2 and TAG-1. *J. Cell Biol.* 162:1149–1160. http://dx.doi.org/10.1083/jcb.200305018

Rasband, M.N., J.S. Trimmer, E. Peles, S.R. Levinson, and P. Shrager. 1999. K+ channel distribution and clustering in developing and hypomyelinated axons of the optic nerve. *J. Neurocytol.* 28:319–331. http://dx.doi.org/10.1023/A:1007057512576

Rhodes, K.J., B.W. Strassle, M.M. Monaghan, Z. Bekele-Arcuri, M.F. Matos, and J.S. Trimmer. 1997. Association and colocalization of the Kvbeta1 and Kvbeta2 beta-subunits with Kv1 alpha-subunits in mammalian brain K+ channel complexes. *J. Neurosci.* 17:8246–8258.

Rios, J.C., C.V. Melendez-Vasquez, S. Einheber, M. Lustig, M. Grumet, J. Hemperly, E. Peles, and J.L. Salzer. 2000. Contactin-associated protein (Caspr) and contactin form a complex that is targeted to the paranodal junctions during myelination. *J. Neurosci.* 20:8354–8364.

Salzer, J.L., P.J. Brophy, and E. Peles. 2008. Molecular domains of myelinated axons in the peripheral nervous system. *Glia*. 56:1532–1540. http://dx.doi.org/10.1002/glia.20750

Sherman, D.L., S. Tait, S. Melrose, R. Johnson, B. Zonta, F.A. Court, W.B. Macklin, S. Meek, A.J. Smith, D.F. Cottrell, and P.J. Brophy. 2005. Neurofascins are required to establish axonal domains for saltatory conduction. *Neuron*. 48:737–742. http://dx.doi.org/10.1016/j.neuron.2005.10.019

Shingai, T., W. Ikeda, S. Kakunaga, K. Morimoto, K. Takekuni, S. Itoh, K. Satoh, M. Takeuchi, T. Imai, M. Monden, and Y. Takai. 2003. Implications of nectin-like molecule-2/IGSF4/RA175/SgIGSF/TSLC1/SynCAM1 in cell-cell adhesion and transmembrane protein localization in epithelial cells. *J. Biol. Chem.* 278:35421–35427. http://dx.doi.org/10.1074/jbc.M305387200

Spiegel, I., K. Adamsky, Y. Eshed, R. Milo, H. Sabanay, O. Sarig-Nadir, I. Horresh, S.S. Scherer, M.N. Rasband, and E. Peles. 2007. A central role for Necl4 (SynCAM4) in Schwann cell-axon interaction and myelination. *Nat. Neurosci.* 10:861–869. http://dx.doi.org/10.1038/nn1915

Susuki, K., and M.N. Rasband. 2008. Spectrin and ankyrin-based cytoskeletons at polarized domains in myelinated axons. *Exp. Biol. Med. (Maywood)*. 233:394–400. http://dx.doi.org/10.3181/0709-MR-243

Tait, S., F. Gunn-Moore, J.M. Collinson, J. Huang, C. Lubetzki, L. Pedraza, D.L. Sherman, D.R. Colman, and P.J. Brophy. 2000. An oligodendrocyte cell adhesion molecule at the site of assembly of the paranodal axo-glial junction. *J. Cell Biol.* 150:657–666. http://dx.doi.org/10.1083/jcb.150.3.657

Terada, N., N. Ohno, S. Saitoh, Y. Saitoh, M. Komada, H. Kubota, and S. Ohno. 2010. Involvement of a membrane skeletal protein, 4.1G, for Sertoli/germ cell interaction. *Reproduction*. 139:883–892. http://dx.doi.org/10.1530/REP-10-0005

Terada, N., Y. Saitoh, N. Ohno, M. Komada, S. Saitoh, E. Peles, and S. Ohno. 2011. Essential function of protein 4.1G in targeting of MPP6 into Schmidt-Lanterman incisures in myelinated nerves. *Mol. Cell. Biol.* 32:199–205. http://dx.doi.org/10.1128/MCB.05945-11

Traka, M., L. Goutebroze, N. Denisenko, M. Bessa, A. Nifli, S. Havaki, Y. Iwakura, F. Fukamauchi, K. Watanabe, B. Soliven, et al. 2003. Association of TAG-1 with Caspr2 is essential for the molecular organization of juxtaparanodal regions of myelinated fibers. *J. Cell Biol.* 162:1161–1172. http://dx.doi.org/10.1083/jcb.200305078

Trapp, B.D., S.B. Andrews, A. Wong, M. O'Connell, and J.W. Griffin. 1989. Co-localization of the myelin-associated glycoprotein and the microfilament components, F-actin and spectrin, in Schwann cells of myelinated nerve fibres. *J. Neurocytol.* 18:47–60. http://dx.doi.org/10.1007/BF01188423

Vabnick, I., J.S. Trimmer, T.L. Schwarz, S.R. Levinson, D. Risal, and P. Shrager. 1999. Dynamic potassium channel distributions during axonal development prevent aberrant firing patterns. *J. Neurosci.* 19:747–758.

Wang, H., D.D. Kunkel, T.M. Martin, P.A. Schwartzkroin, and B.L. Tempel. 1993. Heteromultimeric K+ channels in terminal and juxtaparanodal regions of neurons. *Nature*. 365:75–79. http://dx.doi.org/10.1038/365075a0

Werner, H.B., K. Kuhlmann, S. Shen, M. Uecker, A. Schardt, K. Dimova, F. Orfaniotou, A. Dhaunchak, B.G. Brinkmann, W. Möbius, et al. 2007. Proteolipid protein is required for transport of sirtuin 2 into CNS myelin. *J. Neurosci.* 27:7717–7730. http://dx.doi.org/10.1523/JNEUROSCI.1254-07.2007

Wong, M.H., and M.T. Filbin. 1994. The cytoplasmic domain of the myelin P0 protein influences the adhesive interactions of its extracellular domain. *J. Cell Biol.* 126:1089–1097. http://dx.doi.org/10.1083/jcb.126.4.1089

Wozny, C., J. Breustedt, F. Wolk, F. Varoqueaux, S. Boretius, A.R. Zivkovic, A. Neeb, J. Frahm, D. Schmitz, N. Brose, and A. Ivanovic. 2009. The function of glutamatergic synapses is not perturbed by severe knockdown of 4.1N and 4.1G expression. *J. Cell Sci.* 122:735–744. http://dx.doi.org/10.1242/jcs.037382

Yageta, M., M. Kuramochi, M. Masuda, T. Fukami, H. Fukuhara, T. Maruyama, M. Shibuya, and Y. Murakami. 2002. Direct association of TSLC1 and DAL-1, two distinct tumor suppressor proteins in lung cancer. *Cancer Res.* 62:5129–5133.

Yang, S., H. Weng, L. Chen, X. Guo, M. Parra, J. Conboy, G. Debnath, A.J. Lambert, L.L. Peters, A.J. Baines, et al. 2011. Lack of protein 4.1G causes altered expression and localization of the cell adhesion molecule nectin-like 4 in testis and can cause male infertility. *Mol. Cell. Biol.* 31:2276–2286. http://dx.doi.org/10.1128/MCB.01105-10

Zhou, L., C.L. Zhang, A. Messing, and S.Y. Chiu. 1998. Temperature-sensitive neuromuscular transmission in Kv1.1 null mice: role of potassium channels under the myelin sheath in young nerves. *J. Neurosci.* 18:7200–7215.

Zhou, Y., G. Du, X. Hu, S. Yu, Y. Liu, Y. Xu, X. Huang, J. Liu, B. Yin, M. Fan, et al. 2005. Nectin-like molecule 1 is a protein 4.1N associated protein and recruits protein 4.1N from cytoplasm to the plasma membrane. *Biochim. Biophys. Acta*. 1669:142–154. http://dx.doi.org/10.1016/j.bbamem.2005.01.013